S1 Genetic analyses

Table S1. Summary table of the eight loci applied for the 11 subpopulations from the Taymyr Peninsula, sorted by decreasing population genetic differentiation value F$_{ST}$. Observed and expected heterozygosity are given by HO and HE, respectively.

No.	Locus [1]	Multiplex [2]	TAG [3]	Observed fragment length (bp)	Number of alleles
1	bcLK253	1	Q3	211-247	16.99±0.39
2	Ld101	1	Q4	196-236	15.74±0.79
3	bcLK228	2	Q4	133-269	18.70±0.66
4	bcLK189	3	Q2	152-242	33.39±1.50
5	bcLK211	1	Q2	194-250	22.97±1.09
6	Ld42	3	Q4	187-201	7.86±0.35
7	bcLK056	2	Q1	154-256	31.79±1.05
8	bcLK263	2	Q2	198-280	39.77±0.96

[1] Locus – marker names beginning 'bcLK' are developed by Isoda and Watanabe (2006) and those with 'Ld' by Wagner et al., (2012); [2] Multiplex – number indicates the three primer mixes applied in a simultaneous PCR; [3] TAG - TAG – tailing sequence at forward primer: Q1 = TGTAAAACGACGGCCAGT (Schuelke, 2000); Q2 = TAGGAGTGCAGCAAGCAT; Q3 = CACTGCTTAGAGCGATGC; Q4 = CTAGTTATTGCTCAGCGGT (Q2–Q4, after Culley et al. (2008))).
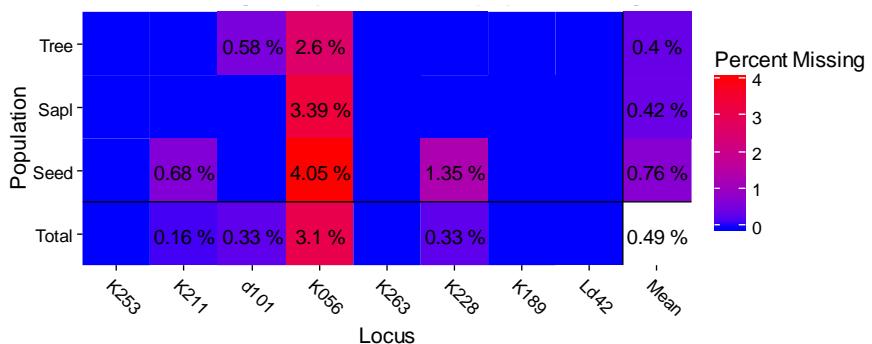
Figure S1. Fraction of missing alleles for each of three height classes – tree, sapling (Sapl), and seedling (Seed) (y-axis) and locus (x-axis) within each height class and the average value.
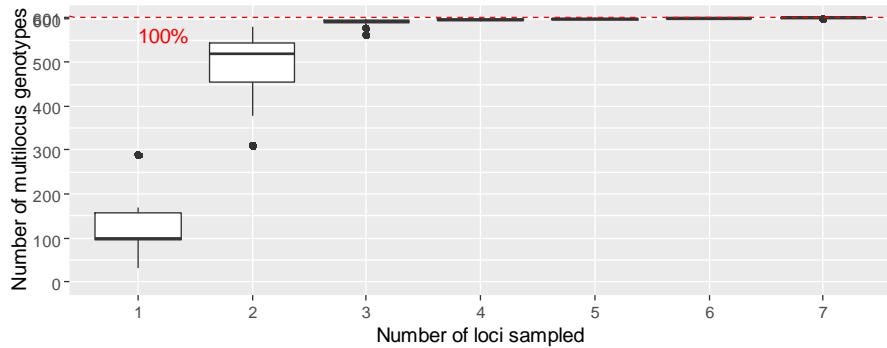
Figure S2. Genotype accumulation curve showing convergence at 5-7 loci from which nearly all 601 tested individuals can be differentiated.

S1.1 Allele diversity

S1.1.1 Introduction
The number of alleles per loci was analysed separately in three height classes: 'seedling' <0.4 m, 'sapling' – taller
25 than seedlings but <2 m, and 'tree' >2 m. For the analyses, we resampled the dataset to avoid errors introduced
by sample size. This was achieved by constructing 100 datasets from 30 randomly selected individuals of each
height class. To check whether the loci were under the null expectation of the Hardy-Weinberg equilibrium, χ^2-
tests were performed on the observed allele frequencies ('hw.test'-function in 'pegas'-library version 0.9 (Paradis,
2010)).

30 To exclude errors introduced by clonal reproduction we used clone-censored datasets for the analyses. By using
all eight loci we could distinguish between all genotyped individuals. We identified 601 separate individuals and
11 clones (Fig. 3a). The members of one genetically identical group were up to 30 m distant from each other;
similar distances were found for black spruce stunted forms (Gamache et al., 2003; Laberge et al., 2000).

S1.1.2 Results
35 The number of alleles per locus was nearly equal among all height classes with two exceptions at locus bcLK189
and bcLK263, at which the allele number was slightly smaller for seedlings. Individuals of all height classes showed
significant heterozygote deficits with an observed mean of ~0.69 and an expected heterozygosity of ~0.86
(p<0.001, Table S2, Figure S4). At two loci (bcLK253 and bcLK263) observed values were close to the expected
ratio and thus did not differ significantly from the Hardy-Weinberg equilibrium (Table S2).

S1.1.3 Discussion
40 The analysed tree stand is characterised by a high gene diversity (number of alleles and expected heterozygosity
of ~86%) compared to other studies which used the same or parts of the same markers (Babushkina et al., 2016;
Oreshkova et al., 2013; Pluess, 2011). Nevertheless, we observe a heterozygote deficit, which results in significant
deviations from Hardy-Weinberg equilibrium, even though the analysed trees grew in a large area (one hectare).
45 This was observed in the treeline area, spanning from dense forest to single-tree stands on the southern Taymyr
Peninsula and which seems to be unaffected by the sampling area (Kruse et al., 2018). In general, this can be
indicative of a higher degree of inbreeding among individuals and thus local recruitment outweighs immigration
(Arenas et al., 2012; Hartl and Clark, 2007), although no straightforward pattern arises from the comparison of
heterozygosity values (mean over all loci) among the three height classes (trees, saplings, seedlings).
50 Nevertheless, in detail, the amount of alleles in seedlings is lower at two loci, for which also the observed
heterozygosity is lower than for the other two height classes. This trend was expected for seedlings at all loci,
because younger cohorts typically show depressed heterozygosity, caused by the higher probability of local
reproduction (Addisalem et al., 2016; Moran and Clark, 2012). Subsequently, due to self-thinning, selection takes
place, generally preferring fitter individuals – assuming heterozygotes are generally fitter (heterosis effect, for
55 example Babushkina et al., 2016) one expects the older an individual is, the fitter it is compared to other
competitors.

Table S2. Heterozygosity values for each locus by height class. The analyses are based on 100 resampled datasets, rarefied to 30 individuals.

Locus	Trees		Saplings		Seedlings	
	HO [%]	HE [%]	HO [%]	HE [%]	HO [%]	HE [%]
Ld101	55.9±8.5	77.4±4.8	53.8±8	79.7±3.8	60.8±8.2	78.8±3.6
bcLK056	62.5±8.9	91±1.4	55.2±8.2	90.1±1.6	64.2±7.4	91±1.1
bcLK189	79.1±6.8	88.8±2	70.2±7	89.3±1.6	72.8±6.5	88.3±1.5
bcLK211	68.6±7.2	88.5±2.5	63.7±6.7	89.4±1.9	66.4±6.7	89.2±1.8
bcLK228	70.8±7.8	87.9±1.6	68.5±7.5	88.4±1.3	65.4±7.5	89±1.4
bcLK253	80.1±8	83.8±2.5	80.3±6.1	83.8±2.6	81.2±6.4	83.3±2.7
bcLK263	90.1±4.8	93.8±0.8	89.6±4.5	93.8±0.7	86.3±5.3	92.6±0.9
Ld42	54.3±8.6	76±3.2	64.3±8.1	74.9±2.9	53±7.8	77.5±2.7
All	**70.2±7.6**	**85.9±2.3**	**68.2±7**	**86.2±2.1**	**68.7±7**	**86.2±2**

60
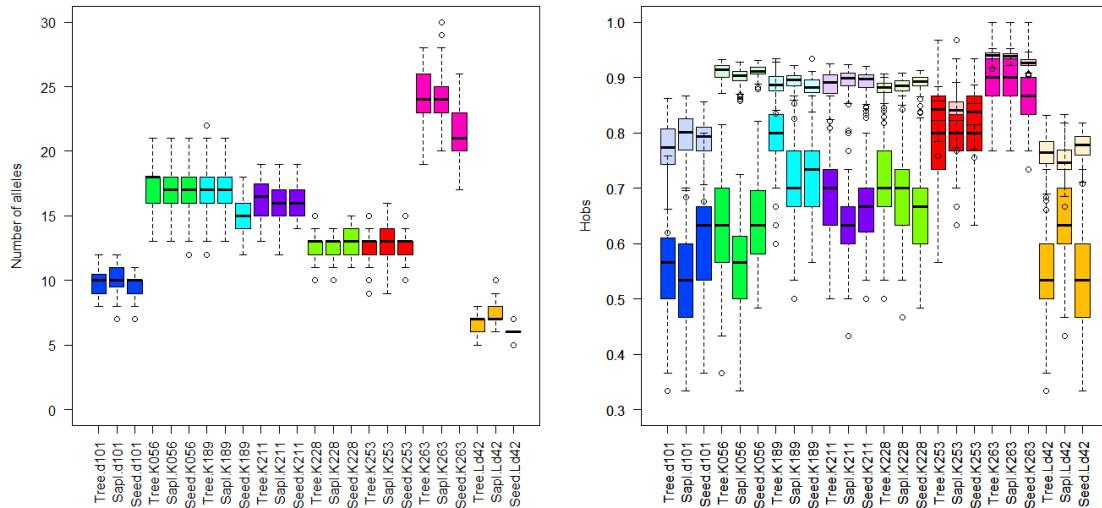
Figure S4. Left: Number of alleles, Right: Observed (H$_O$) and expected (H$_E$) heterozygosity. Based on a rarefied dataset of 30 individuals.
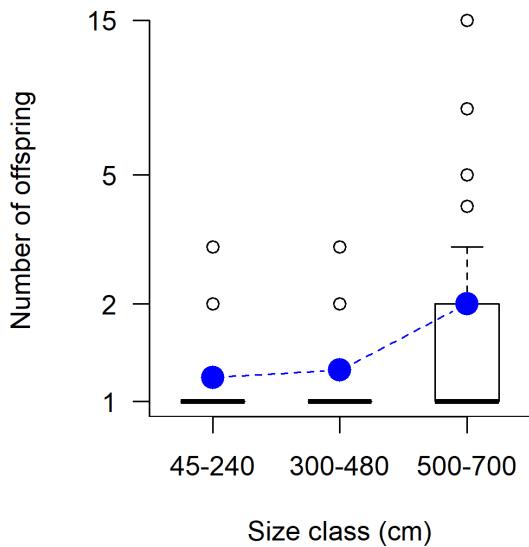
65

Figure S5. Number of offspring assigned to a single parent in three size classes. Filled circles: mean values.

S2 Model adaptation

S2.1 Program code adaptation

S2.1.1 Seed dispersal function improvements

For each dispersed seed the wind direction is randomly drawn from vegetation period wind data of the year of its dispersal. The ballistic maximal flight distance E_0 (Equation 1) is estimated by species-specific size parameters following the approach of Matlack (1987), where V_h is defined as the horizontal wind speed and is chosen correspondingly to the wind direction in the model. The release height H_t is roughly estimated at 75% of the individual's height. V_d is the descent rate for seeds and is estimated for *Larix gmelinii* by a linear regression using species data of Matlack (1987) for species having wing-scales attached to the seeds: $V_d = 0.0032 * \sqrt{w} + 0.4807$ and is 0.86 m s^{-1}, with the wing loading w (Matlack 1987) for *L. gmelinii*, calculated by dividing the average seed weight (in microdyne) of 3.5 mg (Heit and Eliason, 1940; Lukkarinen et al., 2009) by the propagule area of 0.2 cm^2 (Fu et al., 1999).

$$E_0 = V_h \frac{H_t}{V_d} \tag{1}$$

This variable E_0 controls the standard deviation of the Gaussian term in the dispersal function of the model which is named originally '*width*' in Equation 5 in Kruse *et al.* (2016)), consisting of the two dispersal function terms $DL_{gaussian}(rn) = \sqrt{2 * E_0{}^2 * -1 * log(rn)}$ and $DL_{fat-tailed}(rn) = rn^{(-1*(1+\propto))}$, with rn – random number uniformly distributed between 0 and 1, $sdist$ – distance parameter for fitting and $\propto$ - scaling parameter for the fat tail of the function:

$$DL_{gaussian,fat-tail}(rn) = sdist * 0.5 * \left(\left(0.5 * DL_{gaussian}(rn)\right) + \left(2 * DL_{fat-tailed}(rn)\right)\right) \tag{2}$$

S2.1.2 Growth function

The tree growth now depends only on July temperature, because climate-tree ring-width comparisons showed no significant influence of precipitation (data not shown). With the species-specific linear regression coefficients we estimate the simulated tree growth in a year by $julindex = \left(\frac{0.078}{1+e^{14,825-Julytemperature}}\right) + 0.108$, which was further processed to the scale factor $weatherfactor = \frac{julindex-minimalgrowth}{maximalgrowth-minimalgrowth}$.

S2.1.3 Active layer thickness influences mortality

The influence of the active layer thaw depth on the diameter growth of larch trees is estimated based on the results of Nakai *et al.* (2008). It describes a linear relationship allowing 100% diameter growth at 100 cm thaw depth and only 10% when reaching 10 cm, which is the minimum value for *L. gmelinii*. The active layer thickness ALT (Equation 3) is estimated in metres for each year with the Stefan Formula, following simplifications by Hinkel and Nicholas (1995). It is determined by soil properties fe=0.050 (Global Land Cover Characterization, Zhang et al., 2005) and the cumulative sum of daily temperatures exceeding the freezing points DDT:

$$ALT(year) = 1.0 - fe * \sqrt{DDT(year)} \tag{3}$$

Table S4. Overview of model parameters and processes for *L. gmelinii* individuals that differ from the original version (Kruse *et al.* 2016).

Parameter	Value and dimension	References
Growth		
Quadratic term of the equation for diameter growth rate	-0.003 ln(cm) cm^{-2}	data-based estimate similar to Fyllas *et al.* (2010)
Linear term of the growth function	0.030 ln(cm) cm^{-1}	
Constant term of the growth function	-1.98 ln(cm)	
Seed production, dispersal and establishment		
Factor of seed productivity	8	literature-based estimate (Kruklis & Milyutin, 1977, cited in Abaimov, 2010)
Background germination rate	0.01	estimated
Horizontal seed dispersal distance at wind speed of 10 km/h	60.1 m	estimated after Matlack (1987)
Seed descent rate	0.86 m s^{-1}	estimated descent rate based on Matlack (1987)
Mortality		
Background mortality rate	0.0001 yr^{-1}	data-based estimate
Current tree growth influence factor on tree mortality	0.0	estimated
Weather influence factor on tree mortality	0.1	estimated
Density influence factor on tree mortality	2.0	estimated
Seed fertility	2 yrs	Ban *et al.* (1998)
Mean temperature of the coldest month (January) at the border of the species' geographical range	-45 °C	Shugart *et al.* (1992)
Exponent scaling the height influence	0.2	estimated
Weather processing		
Exponent scaling the influence of surrounding density for a tree	0.1	estimated
Exponent scaling the density value	0.5	estimated

S2.2 Simulation results

To explore potential settings (I) to decrease the amount of recruitment close to the mother trees, (II) to shift the
105   effective dispersal peak by 2-3 m and (III) to increase the effective recruitment at medium distances (~30-40 m),
we tuned two kinds of processes: parameters that determine the seed dispersal (model code:
bcdopwxyzDEFGHIJK, Table S5) and tree density and parameters that set the impact of the tree's mortality
(efghijklmnAC), or both (qrstuv) (details on individual adaptations in Table S5).

Of all 36 different simulations, some parameters decreased the amount of near mother effective seed dispersal
110   (I) (cdo-zD-I) of which only (o-z) decreased the distance of up to 2 m based on the shifted dispersal function, while
an increase in the distance parameter of the Gaussian-function peak improves the simulated function strongly
(D-I) (Figure S8). Of these a shift towards farther distances and an increase in medium distances (II+III) was
achieved with adaptations of the dispersal function only (oq-sx-zD-I), whereas the others only shifted the peak to
~5 m with a decrease for medium distances (pt-w). Nevertheless, the sum of squares of deviations from the
115   observed pattern was improved in these candidates by a few sets (yzD-I) to within 66% to 82% of the reference
run. The model performed best with parameter set "I" which is a combination of an adjusted dispersal function
and increased seed production rate (Figure S7, Figure S8, Table S5). These sets increase the distance of dispersed
seeds from the mother tree and the probability of a recruit growing at medium distances from its source was
increased as well. Still the ratio of on-site recruitment was lower than observed (between 45.70 and 46.70
120   compared to observed 56.77%). This was improved by other simulations (qt-wJ) but their general performance
was weaker than the reference simulation.

S2.3 Discussion of the simulation improvement

In parts we achieved a good fit when increasing the peak of the dispersal function in the model to longer distances.
The models where the distance from the centre of the distribution was shifted to 4 m improved the simulated
125   effective seed dispersal distances best ("I"). However, the ratio between on-site recruitment and introductions
from the exterior is around 10% lower than observed. This was not improved by the best-performing parameter
set, but could be improved when changing the density competition, especially for small life stages ("t").
Combinations of both were tested but results were strongly deviated from observed situations ("C"). This smaller
ratio points to an unrealistically high long-distance dispersed seed fraction. Here, we focus on the effective seed
130   dispersal distance at short distances. Nevertheless, long-distance dispersal should be improved too, especially if
one aims to conduct simulation studies over larger extents. It could be improved by decreasing the fat tail
probability of the exponential part in the dispersal function, or by manipulating the implementation of the wind
speed influence to a nonlinear process, decreasing the distances for strong winds. We analysed only one area at
the treeline, which improved our understanding of the processes incorporated in the simulation model, but this
135   may overemphasise the effective seed dispersal of one subpopulation. Therefore further validation by more plot-
based analyses is needed for the general function parameters.

Frequence

Distance to mother [m]
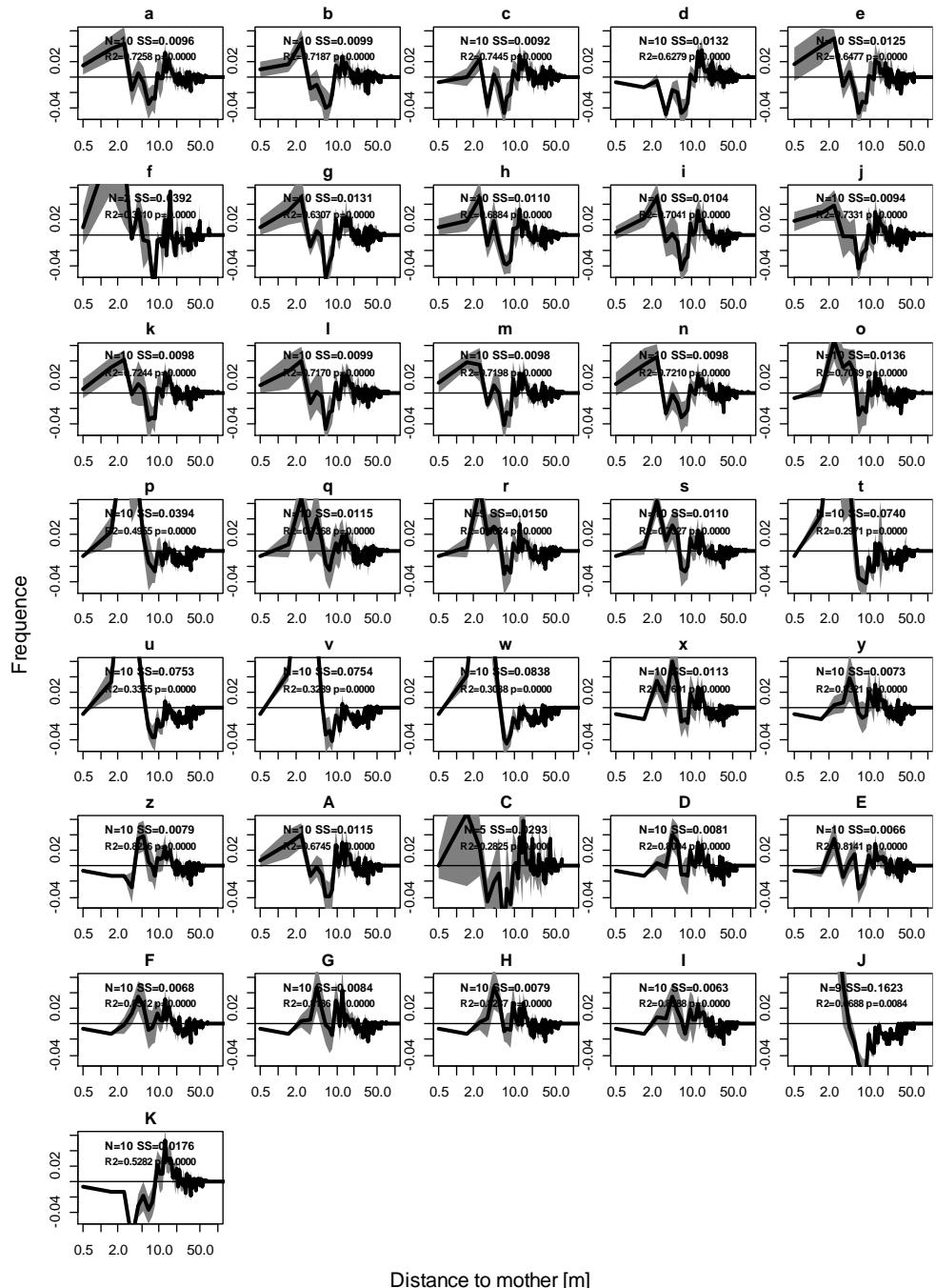
Figure S7. Deviations of simulated versus observed effective seed dispersal. SS – sum of squares, R² – square of
140 **correlation between the mean simulated series and the observed value, p – significance of correlation**
coefficient. Letters (a-zA-K) refer to a special simulation run s. Table S5 for details.
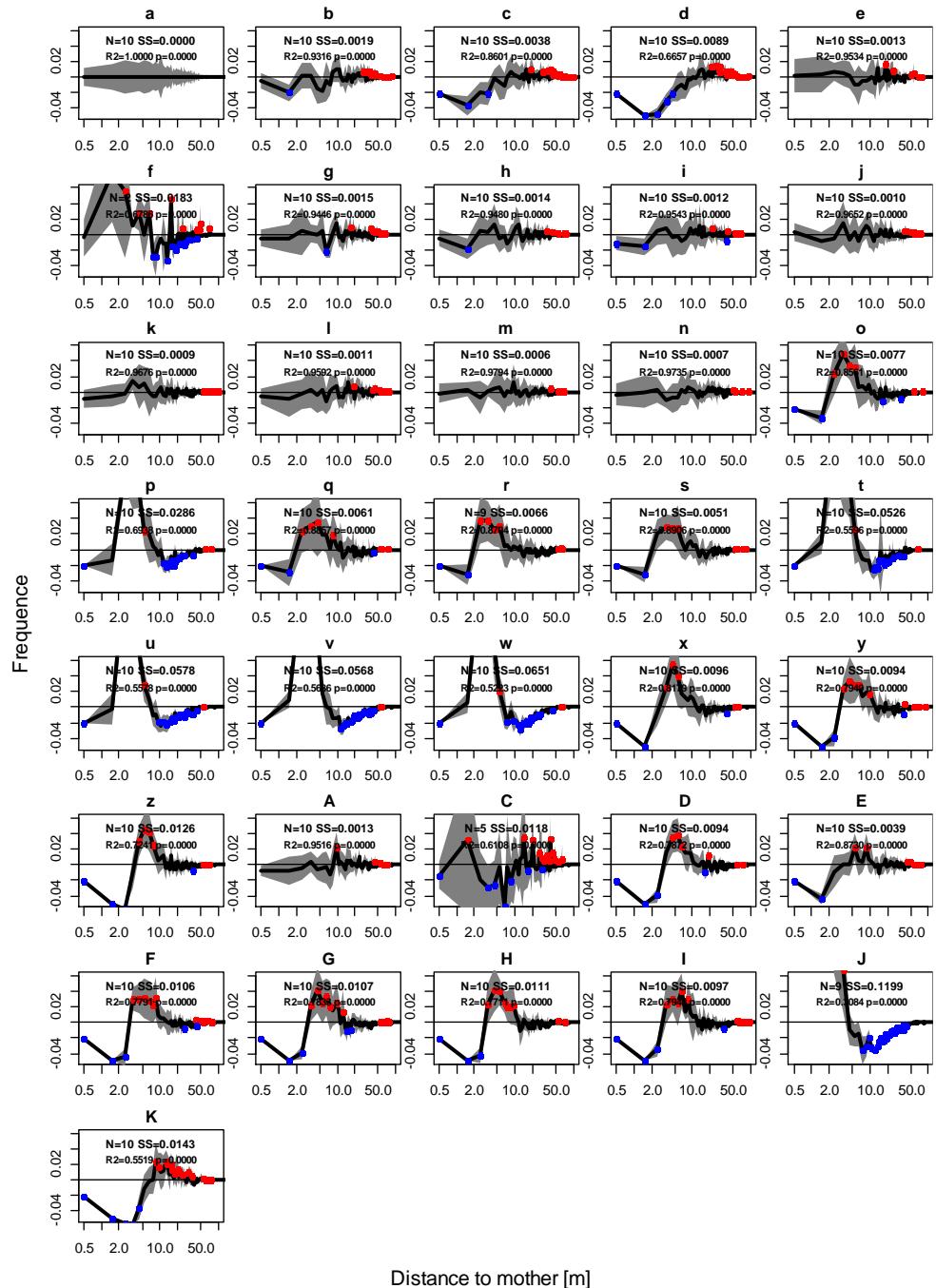
Figure S8. Deviations of effective seed dispersal distances of all runs from the reference simulation "a". Grey areas are the standard deviation of all runs. Red and blue dots indicate values outside (above and below respectively) the standard deviation of the base run. Letters (a-zA-K) refer to a special simulation run s. Table S5 for details.

Table S5. Results of effective seed dispersal in adapted simulations. Changes identifier: 1-dispersal function manipulation, 2-density calculation manipulation, 3-combinations of 1 and 2.

ID	Changes	Dispersal function			On-site recruitment ratio				Model parameters	
		SS	r	r2	Ratio	SD	N>10 in center	p diff from obs	Adaptation and expected outcome	Parameter[1]
a	-	0.0096	0.8519	0.7258	46.8%	1.3%	10	0.0000	- reference run -	Kruse *et al.* (2016)
b	1	0.0099	0.8478	0.7187	45.4%	1.4%	10	0.0000	longer dispersal distances	Sdist=1
c	1	0.0092	0.8629	0.7445	41.0%	1.2%	10	0.0000	longer dispersal distances	Sdist=5
d	1	0.0132	0.7924	0.6279	38.1%	1.0%	10	0.0000	longer dispersal distances	Sdist=10
e	2	0.0125	0.8048	0.6477	46.3%	1.7%	10	0.0000	larger distance to mother trees	mdichte=3
f	2	0.0392	0.5754	0.3310	45.6%	6.7%	3	**0.1023**	smaller distance to mother trees	f_{HAI}=5
g	2	0.0131	0.7942	0.6307	44.8%	2.3%	10	0.0000	larger distance to mother trees	f_{HAI}=15
h	2	0.0110	0.8297	0.6884	45.9%	2.6%	10	0.0000	less exclusion close to mother tree	dichtewertmanipulatorexp=0.05
i	2	0.0104	0.8391	0.7041	48.4%	2.1%	10	0.0000	higher exclusion close to mother tree	dichtewertmanipulatorexp=0.15
j	2	0.0094	0.8562	0.7331	46.2%	1.7%	10	0.0000	higher exclusion close to mother tree	densitysmallweighing=1
k	2	0.0098	0.8511	0.7244	47.0%	1.2%	10	0.0000	less exclusion close to mother tree	densitytreetile=0
l	2	0.0099	0.8467	0.7170	51.5%	2.2%	10	0.0000	higher exclusion close to mother tree	densitytreetile=1
m	2	0.0098	0.8484	0.7198	46.9%	0.7%	10	0.0000	higher exclusion close to mother tree	densitytiletree=1
n	2	0.0098	0.8491	0.7210	47.7%	1.3%	10	0.0000	higher exclusion close to mother tree	densitymaxreduction=1
o	1	0.0136	0.8390	0.7039	47.9%	2.2%	10	0.0000	more distant from centre and more intense peak	Sdist=1 + $r_{GaussExpDisp}$=1.0 + $d_{GaussCentre}$=2.0
p	1	0.0394	0.7039	0.4955	49.9%	3.2%	10	0.0001	shorter dispersal distances	o + $d_{GaussDistance}$=$D*0.5$
q	3	0.0115	0.8584	0.7368	52.0%	2.0%	10	0.0000	higher exclusion close to mother tree	o + densitytreetile=1
r	3	0.0150	0.8139	0.6624	49.3%	2.8%	9	0.0000	less exclusion close to mother tree	o + dichtewertmanipulatorexp=0.15
s	3	0.0110	0.8560	0.7327	44.7%	1.2%	10	0.0000	higher exclusion close to mother tree	o + densitytiletree=3
t	3	0.0699	0.5795	0.3358	52.4%	4.4%	10	**0.0113**	increased tree density	o + treedensity^0.9
u	3	0.0706	0.5957	0.3548	50.9%	2.1%	10	0.0000	increased tree density	o + treedensity^0.95
v	3	0.0788	0.5627	0.3166	51.0%	1.3%	5	0.0006	weakened tree density	o + treedensity^1.1
w	1	0.0838	0.5512	0.3038	52.0%	2.0%	10	0.0000	shortened dispersal distance	o + $d_{GaussDistance}$=$D^{0.5}$
x	1	0.0113	0.8718	0.7601	47.7%	1.4%	10	0.0000	more distant from centre and more intense peak	Sdist=1 + $r_{GaussExpDisp}$=1.0 + $d_{GaussCentre}$=3.0
y	1	0.0073	0.9122	**0.8321**	47.4%	1.3%	10	0.0000	more distant from centre and more intense peak	Sdist=1 + $r_{GaussExpDisp}$=1.0 + $d_{GaussCentre}$=4.0
z	1	0.0079	0.9070	0.8226	46.7%	2.2%	10	0.0000	more distant from centre and more intense peak	Sdist=1 + $r_{GaussExpDisp}$=1.0 + $d_{GaussCentre}$=5.0
A	2	0.0115	0.8213	0.6745	48.6%	2.9%	10	0.0000	higher exclusion close to mother tree	linear density 0-200 cm 1-0 extra mortality
C	2	0.0293	0.5315	0.2825	50.2%	7.5%	7	**0.0613**	higher exclusion close to mother tree	negative quadratic density 0-200 cm 5-0 extra mortality
D	1	0.0081	0.8997	0.8094	45.9%	0.9%	10	0.0000	increased seed production higher on-site reproduction	y + f_s=16 (twice standard)
E	1	**0.0066**	0.9023	0.8141	45.7%	1.8%	10	0.0000	more distant shifted dispersal peak	o + $d_{GaussDistance}$=$D*1.5$
F	1	**0.0068**	0.9226	**0.8512**	46.2%	1.2%	10	0.0000	increased seed production higher on-site reproduction	y + f_s=12
G	1	0.0084	0.9048	0.8186	46.6%	1.6%	10	0.0000	increased seed production higher on-site reproduction	y + f_s=9
H	1	0.0079	0.9103	0.8287	45.7%	1.2%	10	0.0000	increased seed production higher on-site reproduction	y + f_s=10
I	1	**0.0063**	**0.9267**	**0.8588**	46.4%	1.7%	10	0.0000	increased seed production higher on-site reproduction	y + f_s=11
J	1	0.1623	0.2624	0.0688	54.9%	4.0%	9	0.2023	higher on-site reproduction	a + no exponential dispersal
K	1	0.0176	0.7268	0.5282	44.8%	1.3%	10	0.0000	higher on-site reproduction	I + no exponential dispersal

1 – abbreviations following Kruse *et al.* (2016)

150 *References*

Abaimov, A. P.: Permafrost Ecosystems, edited by A. Osawa, O. A. Zyryanova, Y. Matsuura, T. Kajimoto, and R. W. Wein, Springer Netherlands, Dordrecht., 2010.

Addisalem, A. B., Duminil, J., Wouters, D., Bongers, F. and Smulders, M. J. M.: Fine-scale spatial genetic structure in the frankincense tree *Boswellia papyrifera* (Del.) Hochst. and implications for conservation, Tree
155 Genet. Genomes, 12(5), 86, doi:10.1007/s11295-016-1039-2, 2016.

Arenas, M., Ray, N., Currat, M. and Excoffier, L.: Consequences of range contractions and range shifts on molecular diversity, Mol. Biol. Evol., 29(1), 207–218, doi:10.1093/molbev/msr187, 2012.

Babushkina, E. A., Vaganov, E. A., Grachev, A. M., Oreshkova, N. V., Belokopytova, L. V., Kostyakova, T. V. and Krutovsky, K. V.: The effect of individual genetic heterozygosity on general homeostasis, heterosis and resilience
160 in Siberian larch (*Larix sibirica* Ledeb.) using dendrochronology and microsatellite loci genotyping, Dendrochronologia, 38, 26–37, 2016.

Ban, Y., Xu, H., Bergeron, Y. and Kneeshaw, D. D.: Gap regeneration of shade-intolerant Larix gmelini in old-growth boreal forests of northeastern China, J. Veg. Sci., 9(4), 529–536, doi:10.2307/3237268, 1998.

Culley, T. M., Weller, S. G., Sakai, A. K. and Putnam, K. A.: Characterization of microsatellite loci in the Hawaiian
165 endemic shrub *Schiedea adamantis* (Caryophyllaceae) and amplification in related species and genera, Mol. Ecol. Resour., 8(5), 1081–1084, doi:10.1111/j.1755-0998.2008.02161.x, 2008.

Fu, L., Li, N. and Mill, R. R.: Sections on Cephalotaxaceae, Ginkgoaceae and Pinaceae, in Flora of China, edited by W. Zheng-yi and P. H. Raven, pp. 11–52, Science Press; St. Louis: Missouri Botanical Garden, Beijing., 1999.

Fyllas, N. M., Politi, P. I., Galanidis, A., Dimitrakopoulos, P. G. and Arianoutsou, M.: Simulating regeneration and
170 vegetation dynamics in Mediterranean coniferous forests, Ecol. Model., 221(11), 1494–1504, doi:10.1016/j.ecolmodel.2010.03.003, 2010.

Gamache, I., Jaramillo-Correa, J. P., Payette, S. and Bousquet, J.: Diverging patterns of mitochondrial and nuclear DNA diversity in subarctic black spruce: imprint of a founder effect associated with postglacial colonization., Mol. Ecol., 12(4), 891–901 [online] Available from:
175 http://www.ncbi.nlm.nih.gov/pubmed/12753210, 2003.

Hartl, D. L. and Clark, A. G.: Principles Of Population Genetics, 4th ed., Sinauer Associates, Inc. Publishers, Sunderland, Massachusetts, USA., 2007.

Heit, E. C. and Eliason, E. J.: Coniferous tree seed testing and factors affecting germination and seed quality, Tech. Bull. New York State Agric. Exp. Stn., 255, 1–45, 1940.

180 Hinkel, K. M. and Nicholas, J. R. J.: Active layer thaw rate at a boreal forest site in central Alaska, USA, Arct. Alp. Res., 1, 72–80, 1995.

Isoda, K. and Watanabe, A.: Isolation and characterization of microsatellite loci from *Larix kaempferi*, Mol. Ecol. Notes, 6(3), 664–666, doi:10.1111/j.1471-8286.2006.01291.x, 2006.

Kruse, S., Wieczorek, M., Jeltsch, F. and Herzschuh, U.: Treeline dynamics in Siberia under changing climates as
185   inferred from an individual-based model for *Larix*, Ecol. Model., 338, 101–121,
doi:10.1016/j.ecolmodel.2016.08.003, 2016.

Kruse, S., Epp, L. S., Wieczorek, M., Pestryakova, L. A., Stoof-Leichsenring, K. R. and Herzschuh, U.: High gene
flow and complex treeline dynamics of *Larix* Mill. stands on the Taymyr Peninsula (north-central Siberia)
revealed by nuclear microsatellites, Tree Genet. Genomes, 14(2), 19, doi:10.1007/s11295-018-1235-3, 2018.

190   Laberge, M.-J., Payette, S. and Bousquet, J.: Life span and biomass allocation of stunted black spruce clones in
the subarctic environement, J. Ecol., 88, 584–593, 2000.

Lukkarinen, A. J., Ruotsalainen, S., Nikkanen, T. and Peltola, H.: The Growth Rhythm and Height Growth of
Seedlings of Siberian (*Larix sibirica* Ledeb.) and Dahurian (*Larix gmelinii* Rupr.) Larch Provenances in Greenhouse
Conditions, Silva Fenn., 43(1), 5–20, 2009.

195   Matlack, G. R.: Diaspore size, shape, and fall behavior in wind-dispersed plant species, Am. J. Bot., 74(8), 1150–
1160, doi:10.2307/2444151, 1987.

Moran, E. V. and Clark, J. S.: Between-site differences in the scale of dispersal and gene flow in red oak, PLoS
One, 7(5), e36492, doi:10.1371/journal.pone.0036492, 2012.

Nakai, Y., Matsuura, Y., Kajimoto, T., Abaimov, a. P., Yamamoto, S. and Zyryanova, O. a.: Eddy covariance CO2
200   flux above a Gmelin larch forest on continuous permafrost in Central Siberia during a growing season, Theor.
Appl. Climatol., 93(3–4), 133–147, doi:10.1007/s00704-007-0337-x, 2008.

Oreshkova, N. V., Belokon, M. M. and Jamiyansuren, S.: Genetic diversity, population structure, and
differentiation of Siberian larch, Gmelin larch, and Cajander larch on SSR-marker data, Russ. J. Genet., 49(2),
178–186, doi:10.1134/S1022795412120095, 2013.

205   Paradis, E.: Pegas: An R package for population genetics with an integrated-modular approach, Bioinformatics,
26(3), 419–420, doi:10.1093/bioinformatics/btp696, 2010.

Pluess, A. R.: Pursuing glacier retreat: genetic structure of a rapidly expanding *Larix decidua* population, Mol.
Ecol., 20(3), 473–485, doi:10.1111/j.1365-294X.2010.04972.x, 2011.

Schuelke, M.: An economic method for the fluorescent labeling of PCR fragments A poor man's approach to
210   genotyping for research and high-throughput diagnostics., Nat. Biotechnol., 18(February), 233–234, 2000.

Shugart, H. H., Leemans, R. and Bonan, G. B.: A Systems Analysis of the Global Boreal Forest, edited by H. H.
Shugart, R. Leemans, and G. B. Bonan, Cambridge University Press, Cambridge, UK., 1992.

Wagner, S., Gerber, S. and Petit, R. J.: Two highly informative dinucleotide SSR multiplexes for the conifer *Larix
decidua* (European larch)., Mol. Ecol. Resour., 12(4), 717–25, doi:10.1111/j.1755-0998.2012.03139.x, 2012.

215   Zhang, T., Frauenfeld, O. W., Serreze, M. C., Etringer, A., Oelke, C., McCreight, J., Barry, R. G., Gilichinsky, D.,
Yang, D., Ye, H. and others: Spatial and temporal variability in active layer thickness over the Russian Arctic
drainage basin, J. Geophys. Res., 110(D16), D16101, doi:10.1029/2004JD005642, 2005.